RSC Advances

PAPER

Cite this: *RSC Adv.*, 2015, **5**, 11825

A new high-pressure polymeric nitrogen phase in potassium azide†

Meiguang Zhang,*[a] Haiyan Yan,[b] Qun Wei[c] and Hanyu Liu*[d]

To explore new stable polymeric nitrogen phases in alkali metal azides, the crystalline structures of potassium azide KN_3, are systematically investigated up to 400 GPa by using unbiased structure searching methods combined with first principles density functional calculations. Two high-pressure phases of KN_3, insulator *C*2/*m* phase with N^{3-} anions and metallic *P*6/*mmm* phase with "N_6" rings were uncovered above 20 GPa and 41 GPa, respectively, which are consistent with recent theoretical works. Above 274 GPa, a stable *C*2/*m*-N phase featuring polymerized N is identified for the first time and it is energetically much superior to the previously proposed *C*2/*m*-II structure. This *C*2/*m*-N structure consists of zig-zag N polymer nets which can be naturally viewed as the polymerization of "N_6" molecules rings in the low-pressure *P*6/*mmm* phase under increasing pressure. Furthermore, the structure evolutions and accompanied chemical bonding behavior of KN_3 under pressure are also discussed.

Received 3rd December 2014
Accepted 12th January 2015

DOI: 10.1039/c4ra15699d

www.rsc.org/advances

Introduction

Recently, the search for the nonmolecular single-bonded (polymeric) form of solid nitrogen, a typical energy-rich material, has attracted much attention in fundamental science and technological applications. It is known that the polymerization of nitrogen may form a high-energy-density material because the transformation from the weak N–N single bond to extremely strong N≡N triple bond is accompanied by a large energy release (six-fold energy difference, the average bond strength of the N–N single bond is 160 kJ mol^{-1} and that of the triple bond is 954 kJ mol^{-1}), as a consequence of the thermodynamic stability of the product N_2 molecule. The application of high pressure to condensed phases opens an effective route to stabilization of polymeric nitrogen, since pressure can significantly alter the electronic bonding state to modify the physical properties. McMahan and Lesar[1] theoretically predicted that, the molecular N_2 assumes a monatomic polymeric nitrogen phase (cubic gauche structure, called cg-N) above 60 GPa, which was later confirmed in high-pressure (>110 GPa) and high-temperature (>2000 K) experiments by Eremets *et al.*[2,3] More recently, alkali metal azides, constructed by spherical cations and linear molecular N_3^- anions (a straight chain of three nitrogen atoms linked essentially with double N=N bonds), have been proposed to be suitable precursors in the formation of polymeric nitrogen. It could be expected that the N_3^- anion will create polymeric single-covalent-bond networks more easily than diatomic nitrogen, since the N_3^- anion is more weakly bonded than the diatomic triple-bonded nitrogen.[4] Experimentally, the high-pressure structures and N_3^- anion evolution behavior in alkali metal azides LiN_3,[5] NaN_3,[4,6] KN_3,[7,8] RbN_3,[9] and CsN_3 (ref. 10) have been investigated up to 60 GPa, 160 GPa, 55 GPa, 42 GPa, and 55.4 GPa, respectively. In contrast to other azides, the N_3^- anions in NaN_3 were found to transform to a non-molecular nitrogen state with an amorphous-like structure when compressed to 120–160 GPa.[4] Theoretically, previous calculations have predicted the polymerization of nitrogen in LiN_3,[11–13] NaN_3,[14] and CsN_3 (ref. 15) to complement experiments. In our previous works, the N_3^- anions in LiN_3 (ref. 12) and NaN_3 (ref. 14) will all transform to "N_6" molecular clusters and then to a polymerized nitrogen phase above 375 GPa and 152 GPa, respectively.

Potassium azide KN_3, another model system with body-centered tetragonal structure (*I*4/*mcm*, $Z = 2$) at ambient condition, its high-pressure behavior has also been the subject of both experimental and theoretical investigations. Raman scattering up to 4.0 GPa (ref. 16) and X-ray diffraction up to 7.0 GPa (ref. 17) indicate that no phase transition is found in KN_3 these measured pressures. Recent experimental works[7,8] have revealed that a first-order phase transition starts at 13.6 GPa and completes at 32.2 GPa in KN_3 under high pressure. Subsequently, two independent theoretical works performed by Li

[a]*College of Physics and Optoelectronic Technology, Nonlinear Research Institute, Baoji University of Arts and Sciences, Baoji, 721016, China. E-mail: zhmgbj@126.com*
[b]*College of Chemistry and Chemical Engineering, Baoji University of Arts and Sciences, Baoji, 721013, China*
[c]*School of Physics and Optoelectronic Engineering, Xidian University, Xi'an, 710071, China*
[d]*Department of Physics and Engineering Physics, University of Saskatchewan, Saskatoon, S7N5E2, Canada. E-mail: hanyuliu801@gmail.com*

† Electronic supplementary information (ESI) available: See DOI: 10.1039/c4ra15699d

et al.[18] and Zhang *et al.*[19] have reported that the ambient *I*4/*mcm* structure of KN_3 first transforms to a monoclinic *C*2/*m* phase above 20 GPa and then to a metallic hexagonal *P*6/*mmm* phase above 40 GPa. Moreover, Li *et al.*[18] pointed out that the *P*6/*mmm* phase of KN_3 further transform into a polymerized nitrogen structure (named as *C*2/*m*-II phase) above 296.8 GPa. Although this novel polymerized nitrogen *C*2/*m*-II structures proposed, the quest for new energetically stable or metastable polymerized nitrogen structures for KN_3 is still fascinating in view of the wide stable pressure range of *P*6/*mmm* phase (40–296.8 GPa). For this purpose, we here present extensive structure searches to uncover the most energetically stable KN_3 phase up to 400 GPa by means of an Crystal structure AnaLYsis by Particle Swarm Optimization algorithm (CALYPSO)[20,21] in combination with first-principles density functional calculations. This method has been successfully applied to several structures which have been confirmed by independent experiments,[22–24] including the high-pressure experimental structure (HP-I phase) of NaN_3.[14] Indeed, a new polymerized nitrogen phase (*C*2/*m*, $Z = 4$, hereafter denoted as *C*2/*m*-N) is uncovered above 274 GPa, which is energetically much superior to the recent reported candidate *C*2/*m*-II phase. This new polymeric phase consists of zig-zag N polymer nets which can be naturally viewed as the polymerization of "N_6" molecules rings in the low-pressure *P*6/*mmm* phase under increasing pressure. The structure evolutions and accompanied chemical bonding behavior of KN_3 under pressures are also discussed, and these results provide an insight into the formation of polymeric nitrogen in metal azides.

Computational methods

We performed variable-cell high-pressure structure predictions in the range of 0, 25, 50, 100, 200, 300, and 400 GPa with systems containing one to four formula units (f.u.) in simulation cell through CALYPSO code.[20,21] The effectiveness of our method has been demonstrated by recent successes in predicting high-pressure structures of various systems, ranging from elements to binary and ternary compounds.[25–30] The underlying local structural relaxations were performed using the VASP[31,32] code in the framework of density functional theory[33] with the generalized-gradient approximation (GGA) proposed by Perdew–Burke–Ernzerhof (PBE) exchange–correlation functional.[34] The electron and core interactions were included by using the frozen-core all-electron projector augmented wave (PAW) method[35] with N: $2s^2 2p^3$ and K: $3s^2 3p^6 4s^1$ treated as the valence electrons. Tests of the computational parameters showed that energy calculations are well converged to better than 1 meV per atom with a plane-wave energy cutoff of 520 eV and a proper Monkhorst–Pack *k* meshes[36] ($4 \times 15 \times 8$ for *C*2/*m*-N, $6 \times 18 \times 7$ for *C*2/*m*-II, $8 \times 8 \times 15$ for *P*6/*mmm*, $14 \times 14 \times 17$ for *C*2/*m*, and $10 \times 10 \times 10$ for *I*4/*mcm*) in the Brillouin zone. During the geometrical optimization, all forces on atoms were converged to less than 0.001 eV $Å^{-1}$ and the total stress tensor was reduced to the order of 0.01 GPa. The charge density topology was analyzed based on Bader's quantum theory of Atoms-In-Molecules (AIM).[37] The phonon calculations were carried out by using a finite displacement approach through the PHONOPY program.[38]

Results and discussion

At ambient pressure, the ground-state of KN_3 revealed by our *ab initio* structural search is exactly the experimental *I*4/*mcm* structure, validating our method adopted here. For high pressures at 25 GPa and 50–200 GPa, our structure searches uncover the most stable structures to be monoclinic *C*2/*m* phase and hexagonal *P*6/*mmm* phase, respectively, which are consistent with the recent theoretical works.[18,19] Strikingly, the crystal structure and atomic arrangements in this *P*6/*mmm* phase (Fig. 1(a)) of KN_3 is similar to the high-pressure *P*6/*m* phases found in LiN_3 (ref. 11) and NaN_3 (ref. 14) in our previous works. However, as the *P*6/*m* space group indicates, the benzene-like six-membered "N_6" rings layers (Fig. 1(b)) and the *P*6/*mmm* Li(Na) sublattice are not in registry. With increasing pressures of 300 GPa and 400 GPa, a promising monoclinic *C*2/*m*-N phase including partial single N–N bonds was identified for KN_3. Meanwhile, the recent proposed monoclinic *C*2/*m*-II phase[18] (as shown in Fig. 1(c)) was also explored as a metastable phase with respect to the *C*2/*m*-N phase. Fig. 1(d) shows crystal structure of *C*2/*m*-N-KN_3, in which the N atoms adopts a 3D packing consisting of intriguing helical tunnels connected to each other by N–N bonds along the *b*-axis. The structural details of the lattice parameters and the atomic positions of *C*2/*m*-N-KN_3 are listed in Table 1 together with available theoretical results for *P*6/*mmm*-KN_3 and *C*2/*m*-II-KN_3 at different pressures. Inspection further reveals that both N1 and N2 form three covalent bonds with three neighbors and each N3 atom bonding with two neighbors in *C*2/*m*-N-KN_3. In this N atoms helical tunnels presented in Fig. 1(e), the bond lengths of two N neighbors are $d_{N1-N2} = 1.351$ Å, $d_{N1-N3} = 1.267$ Å, and $d_{N2-N3} = 1.281$ Å at 350 GPa, which are close to the three N–N

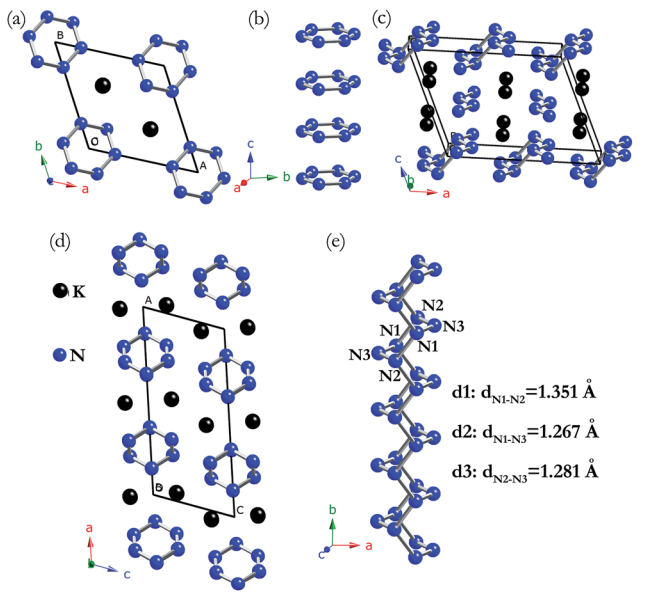

Fig. 1 Crystal structure of *P*6/*mmm*-KN_3 (a), 2D benzene-like "N_6" ring layers along *c*-axis in *P*6/*mmm*-KN_3 (b), crystal structure of *C*2/*m*-II-KN_3 (c), crystal structure of *C*2/*m*-N-KN_3 (d), and 3D "N_6" rings along *b*-axis in *C*2/*m*-N-KN_3 (e). The black and blue spheres represent K and N atoms, respectively.

Table 1 Optimized structural parameters of *P*6/*mmm* phase at 100 GPa, *C*2/*m*-N and *C*2/*m*-II phases at 350 GPa

Phase	Source	Pressure (GPa)	Lattice parameters (Å, °)	Atomic coordinates (fractional)
*P*6/*mmm*	This work	100	$a = b = 5.434$, $c = 2.396$ $\alpha = \beta = 90$, $\gamma = 120$	K 2*d* (0.6667, 0.3333, 0.5) N 6*j* (0.0000, 0.2370, 0.0)
	Ref. 19	100	$a = b = 5.376$, $c = 2.366$ $\alpha = \beta = 90$, $\gamma = 120$	K 2*d* (0.6667, 0.3333, 0.5) N 6*j* (0.0000, 0.2396, 0.0)
	Ref. 18	150	$a = b = 5.202$, $c = 2.259$ $\alpha = \beta = 90$, $\gamma = 120$	K 2*d* (0.6667, 0.3333, 0.5) N 6*j* (0.0000, 0.2440, 0.0)
*C*2/*m*-N	This work	350	$a = 9.654$, $b = 2.177$, $c = 4.326$ $\alpha = \beta = 90$, $\gamma = 108.406$	K 4*m* (0.4556, 0.0, 0.7084) N1 4*m* (0.8262, 0.0, 0.2652) N2 4*m* (0.2441, 0.0, 0.2697) N3 4*m* (0.8588, 0.0, 0.0035)
*C*2/*m*-II	This work	350	$a = 7.603$, $b = 2.120$, $c = 5.834$ $\alpha = \beta = 90$, $\gamma = 112.340$	K 4*i* (0.0621, 1.0, 0.7066) N1 4*i* (0.1798, 0.0, 0.0977) N2 4*i* (0.9115, 0.5, 0.8975) N3 4*i* (0.2056, 0.5, 0.5)
	Ref. 18	350	$a = 7.365$, $b = 2.092$, $c = 5.713$ $\alpha = \beta = 90$, $\gamma = 111.977$	K 4*i* (0.061, 1.0, 0.706) N1 4*i* (0.183, 0.0, 0.097) N2 4*i* (0.911, 0.5, 0.895) N3 4*i* (0.203, 0.5, 0.5)

bond lengths ($d = 1.328$ Å, 1.259 Å, and 1.297 Å) reported in high-pressure polymeric $P2_12_12_1$ structure of nitrogen[39] at same pressure. The dynamical stability of a crystalline structure requires the eigen frequencies of its lattice vibrations be real for all wavevectors in the whole Brillouin zone. We have thus performed the calculations on the phonon dispersion curves of *C*2/*m*-N-KN_3 at 350 GPa. As shown in Fig. 3(a), no imaginary phonon frequency was detected in the whole Brillouin zone for *C*2/*m*-N phase, indicating its dynamical stability at high pressure.

To determine the phase transition pressure of KN_3, the enthalpies of the most predicted energetically stable structures are compared over the studied pressure range as shown in Fig. 2. Fig. 2(a) presents the enthalpy differences of the predicted monoclinic *C*2/*m* phase and hexagonal *P*6/*mmm* phase of KN_3 with respect to the ambient-pressure *I*4/*mcm* phase as a function of pressure up to 60 GPa. It is confirmed that the predicted *C*2/*m* phase structure becomes more stable than the *I*4/*mcm* structure above 20 GPa and is enthalpically stable up to about 41 GPa, above which it transforms to the *P*6/*mmm* structure. These two calculated pressure points for *I*4/*mcm* → *C*2/*m* and *C*2/*m* → *P*6/*mmm* structural phase transitions are in excellent agreement with the recent theoretical works.[18,19] Meanwhile, the dependence of volume on pressure is shown in the inset of Fig. 2(a). The results suggest that both *I*4/*mcm* → *C*2/*m* and *C*2/*m* → *P*6/*mmm* phase transitions are first-order with volume drops of 1.8% and 8.9%, which can be easily detected in further experiments. Fig. 2(b) shows the enthalpy curves of our new predicted polymerized nitrogen *C*2/*m*-N phase relative to the *P*6/*mmm* phase, and the previous reported *C*2/*m*-II phase was also considered for comparison. It can be seen that *C*2/*m*-N-KN_3 becomes more stable than the *P*6/*mmm*-KN_3 above 274 GPa. Compared to the *C*2/*m*-N-KN_3, the *C*2/*m*-II-KN_3 possesses larger enthalpy values in the studied pressure ranges from 200 GPa to 500 GPa and thus appear to be a metastable phase. In addition, the thermodynamic stability of *C*2/*m*-N-KN_3 at concerned pressure range (100–500 GPa) was examined in terms of the formation enthalpies of the reaction route: $\Delta H_f = H_{KN_3} - H_K - \frac{3}{2}H_{N_2}$, where the *dhcp*-K[40] and *Pba*2-N_2 (ref. 39) were chosen as the reference phases. The calculated formation enthalpies indicate that the formation of the KN_3 is exothermic at the studied pressure range. Thus the KN_3 crystal keeps stable against decomposition into the mixture of K + N_2. The calculated *P*–*V* curves (the inset of Fig. 2(b)) of these two high-pressure structures suggested that the phase transitions of *P*6/*mmm* → *C*2/*m*-N is also first-order with volume reduction of 4.2%. The remarkable reconstitution of nitrogen networks in *P*6/*mmm* → *C*2/*m*-N phase transition can naturally explained the pressure effect on the polymerization of nitrogen in KN_3. As shown in Fig. 1(a) and (b), the six N atoms within the *P*6/*mmm* phase form a benzene-like "N_6" ring layers, K and N layers are localized in different layers and construct an intriguing N–K–N sandwiches structure. With increasing pressure above 274 GPa, the planar "N_6" rings in low-pressure *P*6/*mmm* phase were strongly distorted and formed a dense 3D puckered "N_6" rings network connected by N1–N2 bonds (see Fig. 1(e)) with concomitant displacement of K atoms in high-pressure *C*2/*m*-N phase. While the dimensionality of the nitrogen covalent bond network in KN_3 from 2D to 3D as pressure increases, there is a trend of decreasing local symmetry of nitrogen atoms in the structural sequence *P*6/*mmm* → *C*2/*m*-N. These results may provide value implications for the formation of polymeric nitrogen in other metal azides.

The rearrangement of atoms is always accompanied by a notable change of properties for solids, especially for electronic properties. To explore that, we have calculated the total and site projected density of states (DOS), band structure, and Electronic Localization Function (ELF)[41] distributions of *P*6/*mmm*-KN_3 and *C*2/*m*-N-KN_3 at 100 GPa and 350 GPa, respectively. Consensus have been reached[18,19] on that both ambient-pressure *I*4/*mcm* and high-pressure *C*2/*m* structures of KN_3 exhibit insulating characters in their stable pressure range and thus are not shown here. As shown in Fig. 3(b) and (c), the screened hybrid density functional as proposed by Heyd, Scuzeria, and Ernzerhof (HSE06)[42]

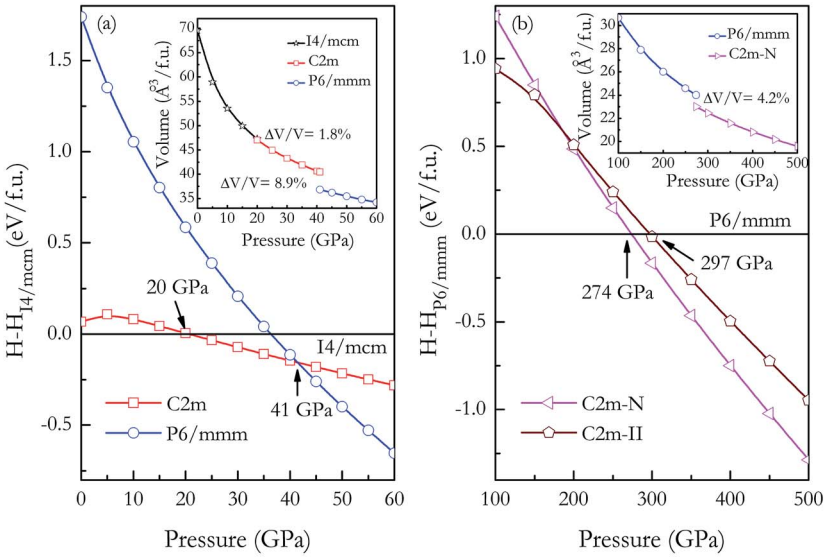

Fig. 2 Enthalpies differences of $C2/m$-KN_3 and $P6/mmm$-KN_3 relative to ambient-pressure $I4/mcm$-KN_3 as a function of pressure (a) and enthalpy differences for $C2/m$-N-KN_3 relative to $P6/mmm$-KN_3 as a function of pressure (b).

is employed to investigate the band structures and density of states of $P6/mmm$-KN_3 and $C2/m$-N-KN_3. For $P6/mmm$-KN_3 at 100 GPa in Fig. 3(b), one can see that the HSE06 calculated band structures cross the Fermi level along Γ → A, H → K, M → L directions in the Brillouin zone, indicating its metallic character. However, Fig. 3(c) presents that the $C2/m$-N-KN_3 is a semiconductor characterized by an indirect band gap of ~1.59 eV. Therefore, the pressure-induced phase transition sequences of $C2/m$ → $P6/mmm$ and $P6/mmm$ → $C2/m$-N for KN_3 are accompanied by metal–semiconductor transitions, first from insulating to metallic state at 41 GPa and then from metallic back to semiconducting state at 274 GPa. This unusual change of the electronic structure of KN_3

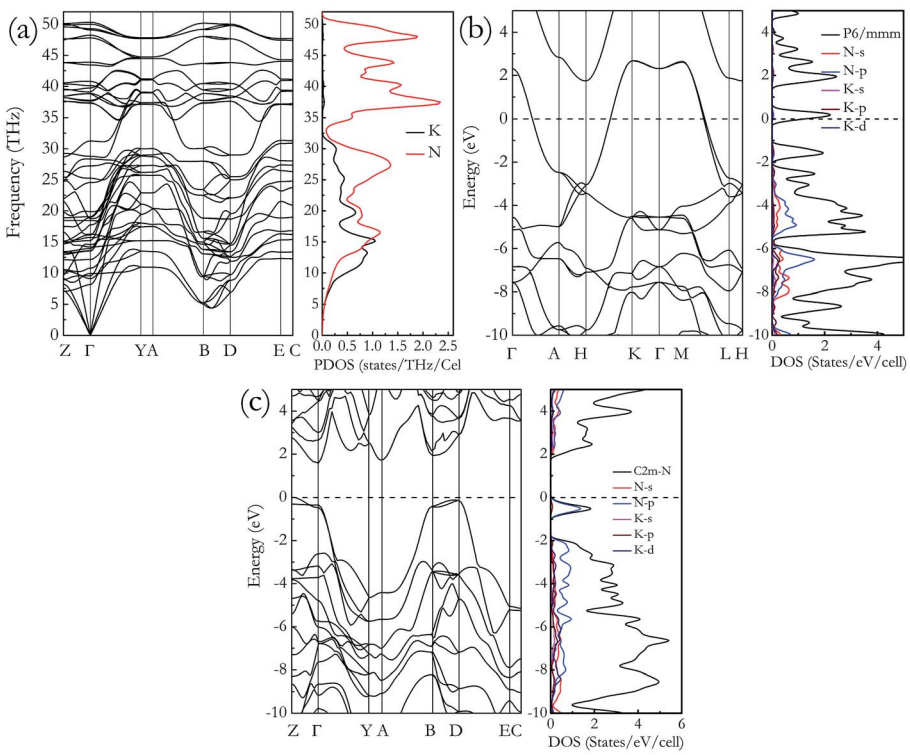

Fig. 3 Phonon dispersion curves of $C2/m$-N-KN_3 at 350 GPa (a), the band structure and density of states of $P6/mmm$-KN_3 at 100 GPa (b), and the band structure and density of states of $C2/m$-N-KN_3 at 350 GPa (c). The horizontal dashed lines denote the Fermi level.

under pressure is similar to that found in LiN_3.[12] The atom-resolved DOS of *P*6/*mmm* and *C*2/*m*-N structures reveal that the densities of states near Fermi levels are mainly originated form the N orbitals electrons. As reported in previous work,[19] the benzene-like "N_6" rings in the *P*6/*mmm*-KN_3 indicates that the N atoms are in sp^2 hybridization and each N atom forms two σ bonds with two neighboring N atoms. The extra sp^2 orbitals are also filled and form the lone pairs, as shown in Fig. 4(a). We found through Bader charge analysis that the charge transfer from K to N atom is 0.76e in one f.u., signifying the K–N ionic bonding nature. This means that the N_6^{2-} anion in *P*6/*mmm* phase has nearly 8 π-electrons. Six P_z orbitals form three π bonding orbitals and three π antibonding orbitals. Thus, the π antibonding orbitals are partially occupied by two electrons, accompanied by two conduction bands crossing the Fermi level as shown in Fig. 3(b). In the 3D puckered "N_6" rings network of *C*2/*m*-N-KN_3 shown in Fig. 1(e), all N1 and N2 atoms are in the sp^3 hybridization and form three N–N σ bonds with neighboring N atoms and one lone pair. The N3 atoms in this puckered rings form two N–N σ bonds with neighboring N atoms and two lone pairs. The strong covalent bondings between different inequivalent N atoms as well as the lone pairs on the side N atoms are also revealed by the ELF (Fig. 4(b)). Therefore, all the bonding states and lone pair states are filled and all the anti-bonding states are unoccupied in *C*2/*m*-N-KN_3, leading to a semiconducting state.

The nature of chemical bonding in *P*6/*mmm*-KN_3 and *C*2/*m*-N-KN_3 at 100 GPa and 350 GPa were further studied through a topological analysis of charge density using the Bader atoms-in-molecules (AIM) method at HSE06 functionals level. The basic idea of AIM analysis is to extract bonding information from the electron density $\rho(\boldsymbol{r})$. The analysis of its electron density gradient $\nabla\rho(\boldsymbol{r})$ helps to define an atom within a molecule or solid through the "zero-flux surface" condition. The analysis of the electron density extrema, *i.e.*, at critical points, located at $\boldsymbol{r}_{CP}$ for which $\nabla\rho(\boldsymbol{r}_{CP})$, allows the characterization of the nature of bonding.[43] The (3, −1) bond critical points (BCPs) which locate at the adjacent nitrogen atoms ($d_{N-N} = 1.288$ Å) within pseudo-benzene "N_6" ring possess negative $\nabla^2\rho(\boldsymbol{r}_{CP})$ (Laplacian value) and large $\rho(\boldsymbol{r}_{CP})$ (local electronic density of 2.967 eÅ^{-3}), indicating the strong double N=N covalent bonding nature. However, $\rho(\vec{\boldsymbol{r}}_{CP})$ of inter-"N_6" BCPs are much smaller (*i.e.* 0.263 eÅ^{-3}) and the corresponding $\nabla^2\rho(\vec{\boldsymbol{r}}_{CP})$ are positive, suggesting closed shell interaction among these "N_6" rings. For *C*2/*m*-N-KN_3 at 350 GPa, both BCPs located between N2–N3 (1.281 Å) and N1–N3 atoms (1.267 Å) exhibit negative $\nabla^2\rho(\boldsymbol{r}_{CP})$ and large $\rho(\boldsymbol{r}_{CP})$ of 3.033 and 3.133 eÅ^{-3}, which are little larger than that of adjacent nitrogen atoms within "N_6" ring in low-pressure *P*6/*mmm* structure. As expected, the BCPs sitting between N1 and N2 atoms have relative smaller value of local density $\rho(\boldsymbol{r}_{CP})$ (2.662 eÅ^{-3}) due to its longer bond length of 1.351 Å, which is consistent with its three-fold coordinated environment. The BCPs of unequivalent N and K atoms in *P*6/*mmm*-KN_3 and *C*2/*m*-N-KN_3 are all positive, indicating closed shell interaction character which is in agreement with an "ionized" K picture presented in the partial DOS (Fig. 3(b) and (c)).

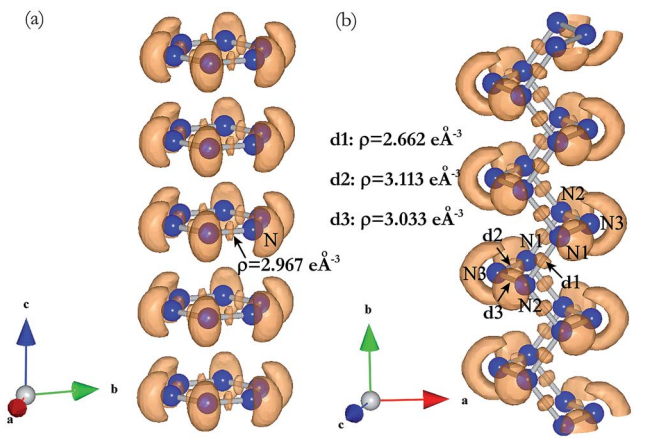

Fig. 4 The ELF distributions of 2D "N_6" rings along *c*-axis in *P*6/*mmm*-KN_3 (a) and 3D "N_6" rings along *b*-axis in *C*2/*m*-N-KN_3. The electron densities located at different (3, −1) bond critical points (BCPs) in 2D "N_6" rings and 3D "N_6" rings are also presented.

Conclusions

In summary, an unbiased structure search method in combination with first-principles calculations was employed to explore the high-pressure polymeric nitrogen phase of KN_3 up to 400 GPa. For the first time, we identify a novel monoclinic *C*2/*m*-N phase featuring 3D polymerized nitrogen above 274 GPa, and this new polymeric nitrogen phase is energetically much superior to the previously proposed *C*2/*m*-II structure. Phonon dispersion and formation enthalpies calculations suggest that *C*2/*m*-N is dynamically stable and is stable against the decomposition into the structure mixture of K + N_2 at high pressure. The analysis of the electronic structure reveals that the polymerization of nitrogen from 2D "N_6" molecular rings to 3D puckered "N_6" rings network in KN_3 is driven by hybridization of N atomic orbitals, which changes from sp^2 to sp^3 under very high pressure.

Acknowledgements

This work was financially supported by the Natural Science Foundation of China (no. 11204007) and Natural Science Basic Research plan in Shaanxi Province of China (grant no. 2012JQ1005).

References

1 A. K. McMahan and R. Lesar, *Phys. Rev. Lett.*, 1985, **54**, 1929.
2 M. I. Eremets, A. G. Gavriliuk, I. A. Trojan, D. A. Dzivenko and R. Boehler, *Nat. Mater.*, 2004, **3**, 558.
3 M. I. Eremets, A. G. Gavriliuk and I. A. Trojan, *Appl. Phys. Lett.*, 2007, **90**, 171904.
4 M. I. Eremets, M. Y. Popov, I. A. Trojan, V. N. Denisov, R. Boehler and R. J. Hemley, *J. Chem. Phys.*, 2004, **120**, 10618.

5 S. A. Medvedev, I. A. Trojan, M. I. Eremets, T. Palasyuk, T. M. Klapötke and J. Evers, *J. Phys.: Condens. Matter*, 2009, **21**, 195404.
6 H. Y. Zhu, F. X. Zhang, C. Ji, D. B. Hou, J. Z. Wu, T. Hannon and Y. Z. Ma, *J. Appl. Phys.*, 2013, **113**, 033511.
7 C. Ji, F. X. Zhang, D. B. Hou, H. Y. Zhu, J. Z. Wu, M.-C. Chyu, V. I. Levitas and Y. Z. Ma, *J. Phys. Chem. Solids*, 2011, **72**, 736.
8 C. Ji, R. Zheng, D. B. Hou, H. Y. Zhu, J. Z. Wu, M.-C. Chyu and Y. Z. Ma, *J. Appl. Phys.*, 2012, **111**, 112613.
9 D. M. Li, X. X. Wu, J. R. Jiang, X. L. Wang, J. Zhang, Q. L. Cui and H. Y. Zhu, *Appl. Phys. Lett.*, 2014, **105**, 071903.
10 D. B. Hou, F. X. Zhang, C. Ji, T. Hannon, H. Y. Zhu, J. Z. Wu and Y. Z. Ma, *Phys. Rev. B: Condens. Matter Mater. Phys.*, 2011, **84**, 064127.
11 M. G. Zhang, H. Y. Yan, Q. Wei, H. Wang and Z. J. Wu, *Europhys. Lett.*, 2013, **101**, 26004.
12 X. L. Wang, J. F. Li, J. Botana, M. G. Zhang, H. Y. Zhu, L. Chen, H. M. Liu, T. Cui and M. S. Miao, *J. Chem. Phys.*, 2013, **139**, 164710.
13 D. L. V. K. Prasad, N. W. Ashcroft and R. Hoffmann, *J. Phys. Chem. C*, 2013, **117**, 20838.
14 M. G. Zhang, K. T. Yin, X. X. Zhang, H. Wang, Q. Li and Z. J. Wu, *Solid State Commun.*, 2013, **161**, 23.
15 X. L. Wang, J. F. Li, H. Y. Zhu, L. Chen and H. Q. Lin, *J. Chem. Phys.*, 2014, **141**, 044717.
16 C. W. Christoe and Z. Iqbal, *Chem. Phys. Lett.*, 1976, **39**, 511.
17 C. E. Weir, S. Block and G. J. Piermarini, *J. Chem. Phys.*, 1970, **53**, 4265.
18 J. F. Li, X. L. Wang, N. Xu, D. Y. Li, D. C. Wang and L. Chen, *Europhys. Lett.*, 2013, **104**, 16005.
19 J. Zhang, Z. Zeng, H. Q. Lin and Y. L. Li, *Sci. Rep.*, 2014, **4**, 4358.
20 Y. C. Wang, J. Lv, L. Zhu and Y. M. Ma, *Phys. Rev. B: Condens. Matter Mater. Phys.*, 2010, **82**, 094116.
21 Y. C. Wang, J. Lv, L. Zhu and Y. M. Ma, *Comput. Phys. Commun.*, 2012, **183**, 2063.
22 L. Zhu, H. Wang, Y. C. Wang, J. Lv, Y. M. Ma, Q. L. Cui, Y. M. Ma and G. T. Zou, *Phys. Rev. Lett.*, 2011, **106**, 145501.
23 J. Lv, Y. C. Wang, L. Zhu and Y. M. Ma, *Phys. Rev. Lett.*, 2011, **106**, 015503.
24 D. N. Hamane, M. G. Zhang, T. Yagi and Y. M. Ma, *Am. Mineral.*, 2012, **97**, 568.
25 L. Zhu, H. Y. Liu, C. J. Pickard, G. T. Zou and Y. M. Ma, *Nat. Chem.*, 2014, **6**, 644.
26 Y. C. Wang, H. Y. Liu, J. Lv, L. Zhu, H. Wang and M. Y. Ma, *Nat. Commun.*, 2011, **2**, 563.
27 H. Wang, J. S. Tse, K. Tanaka, T. Iitaka and Y. M. Ma, *Proc. Natl. Acad. Sci. U. S. A.*, 2012, **109**, 6463.
28 X. L. Wang, Y. C. Wang, M. S. Miao, X. Zhong, J. Lv, T. Cui, J. F. Li, L. Chen, C. J. Pickard and Y. M. Ma, *Phys. Rev. Lett.*, 2012, **109**, 175502.
29 F. Peng, M. S. Miao, H. Wang, Q. Li and Y. M. Ma, *J. Am. Chem. Soc.*, 2012, **134**, 18599.
30 Q. Li, D. Zhou, W. T. Zheng, Y. M. Ma and C. F. Chen, *Phys. Rev. Lett.*, 2013, **110**, 136403.
31 G. Kresse and D. Joubert, *Phys. Rev. B: Condens. Matter Mater. Phys.*, 1999, **59**, 1758.
32 G. Kresse and J. Furthmüller, *Phys. Rev. B: Condens. Matter Mater. Phys.*, 1996, **54**, 11169.
33 W. Kohn and L. J. Sham, *Phys. Rev.*, 1965, **140**, A1133.
34 J. P. Perdew, K. Burke and M. Ernzerhof, *Phys. Rev. Lett.*, 1996, **77**, 3865.
35 P. E. Blöchl, *Phys. Rev. B: Condens. Matter Mater. Phys.*, 1994, **50**, 17953.
36 H. J. Monkhorst and J. D. Pack, *Phys. Rev. B: Solid State*, 1976, **13**, 5188.
37 R. F. W. Bader, *Acc. Chem. Res.*, 1985, **18**, 9.
38 A. Togo, F. Oba and I. Tanaka, *Phys. Rev. B: Condens. Matter Mater. Phys.*, 2008, **78**, 134106.
39 Y. M. Ma, A. R. Oganov, Z. W. Li, Y. Xie and J. Kotakoski, *Phys. Rev. Lett.*, 2009, **102**, 065501.
40 Y. M. Ma, A. R. Oganov and Y. Xie, *Phys. Rev. B: Condens. Matter Mater. Phys.*, 2009, **78**, 014102.
41 A. D. Becke and K. E. Edgecombe, *J. Chem. Phys.*, 1990, **92**, 5397.
42 A. V. Krukau, O. A. Vydrov, A. F. Izmaylov and G. E. Scuseria, *J. Chem. Phys.*, 2006, **125**, 224106.
43 J. S. Tse, Y. S. Yao, D. D. Klug and S. Desgreniers, *J. Phys.: Conf. Ser.*, 2008, **121**, 012006.